Toric Mutations in the dP_2 Quiver

Yibo Gao[1], Zhaoqi Li[2], Thuy-Duong Vuong[1], Lisa Yang[1]

[1]Massachusetts Institute of Technology, [2]Macalester College

MACALESTER COLLEGE

Motivation

Cluster Algebras have rich applications in algebraic combinatorics, tropical geometry, and representation theory. It is common to picture a cluster as a quiver with a cluster variable on each vertex. In this research, we examine the del Pezzo 2 (dP_2) quiver, which arise from physics literature. We classify all cluster variables generated by toric mutations and give combinatorial interpretations for them.

Introduction

We first introduce some basic concepts and our main focus, the dP_2 quiver, which is the left directed graph of Figure 1.

Definition 1.1. A *toric mutation* at some vertex i with in-degree 2 and out-degree 2 corresponds to the following actions on the quiver (i.e. a digraph):

- For every 2-path through i (e.g. $j \to i \to k$), add an edge from j to k.
- Reverse the directions of the arrows incident to i.
- Delete any 2-cycles created from the previous two steps (An example is shown in Figure 1).

Binomial Exchange Relation $\quad x_1' = \frac{x_2x_5+x_3x_4}{x_1}$.

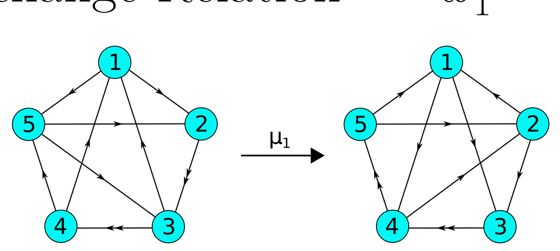

Figure 1: Examples of a Toric Mutation

The dP_2 quiver has two models that can be reached from the original quiver by toric mutations, as is shown in Figure 2.

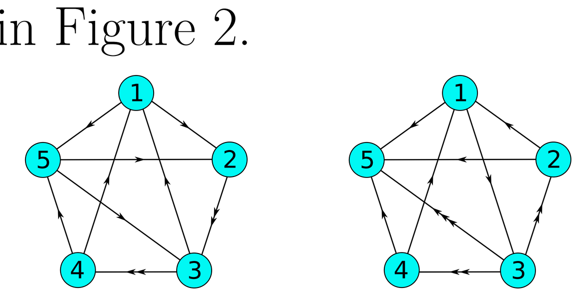

Figure 2: Model 1 (left) and Model 2 (right) of the dP2 quiver

Definition 1.2. *Brane tilings* are infinite, bipartite, periodic, planar graphs that are dual to quivers. Figure 3 shows the corresponding dP_2 brane tiling.

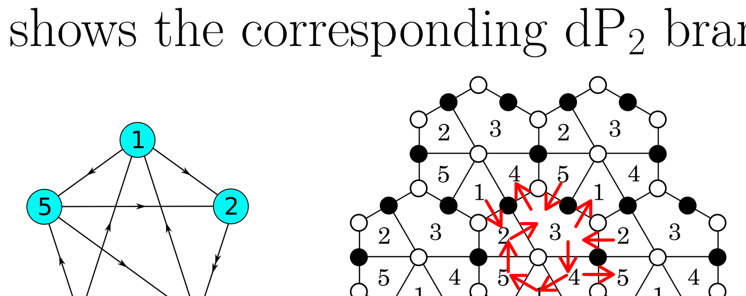

Figure 3: dP2 quiver and its corresponding brane tiling

Toric Mutation Sequences

Definition 2.1. [ρ-mutations] $\quad \rho_1 = \mu_1 \circ (54321)$,

$\rho_2 = \mu_5 \circ (12345)$, $\quad \rho_3 = \mu_2 \circ \mu_4 \circ (24)$,

$\rho_4 = \mu_2 \circ \mu_1 \circ \mu_4 \circ (531)$, $\quad \rho_5 = \mu_4 \circ \mu_5 \circ \mu_2 \circ (351)$,

$\rho_6 = \mu_2 \circ \mu_1 \circ \mu_2 \circ (531)(24)$, $\quad \rho_7 = \mu_4 \circ \mu_5 \circ \mu_4 \circ (135)(24)$.

Example 2.2. Figure 4 shows an example of ρ_1.

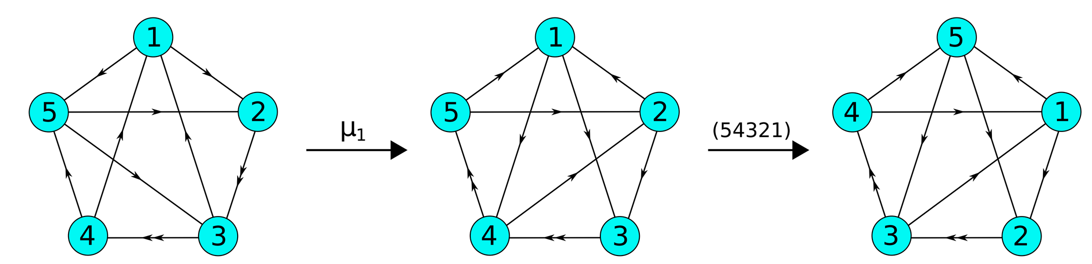

Figure 4: An Example of $\rho-$mutation Sequence

These $\rho-$mutations all fix the quiver, but not the cluster variables. We use these mutation sequences later to derive the formula for cluster variables.

Also, the combinations of these $\rho-$mutation sequences give all possible mutation sequences that start in model 1 and end in model 1, as is shown in Figure 5.

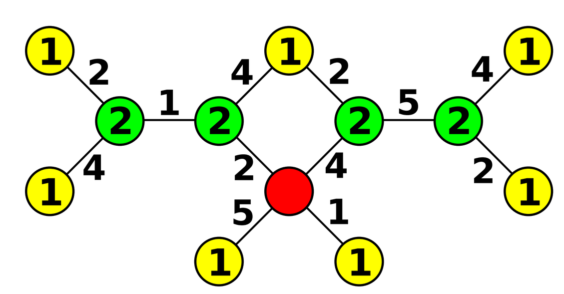

Figure 5: All possible toric mutation sequences from model 1 to model 1.

Furthermore, those combinations can be written in certain form, as is shown in Theorem 2.3.

Theorem 2.3. Every toric mutation sequence that starts at the original dP_2 quiver and ends in model 1 can be written as either

$$\rho_1^k(\rho_3\rho_1)^m \quad \text{or} \quad \rho_1^k(\rho_3\rho_1)^m\rho_3,$$

where $k \in \mathbb{Z}$, $m \in \mathbb{Z}_{\geq 0}$ and $\rho_1^{-1} = \rho_2$.

Formula for Cluster Variables

Theorem 3.2 gives an explicit formula for all cluster variables generated by ρ-mutations, which characterizes them into two categories, as is stated in Corollary 3.3.

Definition 3.1. [Some Constants]

$$A := \frac{x_1x_5 + x_3^2}{x_2x_4}, \qquad B := \frac{x_1x_4^2 + x_2x_3x_4 + x_2^2x_5}{x_1x_3x_5}.$$

Theorem 3.2. Define $g(s,k) := \lfloor \frac{s}{2} \rfloor \lfloor \frac{s+1}{2} \rfloor$ if k is even and $g(s,k) := \lfloor \frac{s-1}{2} \rfloor \lfloor \frac{s}{2} \rfloor$ if k is odd. Then we have, for $k \in \mathbb{Z}$ and $s \in \mathbb{Z}_{\geq 0}$,

$$\rho_1^k(\rho_3\rho_1)^s\{x_1,x_2,x_3,x_4,x_5\} = \{A^{g(s+1,k)}B^{g(s+1,k+1)}x_{k+s+1}, A^{g(s,k)}B^{g(s,k+1)}x_{k+s+2}, A^{g(s+1,k)}B^{g(s+1,k+1)}x_{k+s+3}, A^{g(s,k)}B^{g(s,k+1)}x_{k+s+4}, A^{g(s+1,k)}B^{g(s+1,k+1)}x_{k+s+5}\}.$$

Corollary 3.3. All cluster variables generated by toric mutations can be written as $A^{n^2}B^{n(n-1)}x_{2m}$ or $A^{n(n-1)}B^{n^2}x_{2m-1}$ for some $m, n \in \mathbb{Z}$.

Subgraphs of the Brane Tiling

In the dP_2 brane tiling, for each cluster variable, we seek for a corresponding subgraph whose weight equals the variable, which gives a combinatorial interpretation. To connect cluster variables with subgraphs, we use the weighting scheme utilized in [1] and [2]. Definition 4.1 gives a visualization of it.

Definition 4.1. [Weight Scheme]

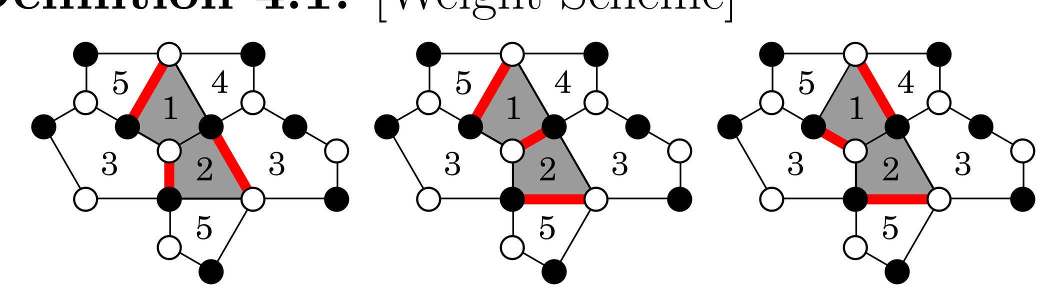

Figure 6: $w(G) = \frac{1}{x_1x_5x_2^2x_3^2} + \frac{1}{x_1^2x_5^2x_2^2} + \frac{1}{x_1^2x_2x_3x_4x_5}$

Main Theorem

Theorem. [Formula of Contours] Define the contours as follows:

$$A^{n^2}B^{n^2-n}x_{2k} = \left(k-2+n, -\left\lceil \frac{k-4+5n}{2} \right\rceil, 2n-1, \left\lfloor \frac{k-3n}{2} \right\rfloor, 1+n-k\right)$$

$$A^{n^2+n}B^{n^2}x_{2k-1} = \left(k-2+n, -\left\lceil \frac{k-2+5n}{2} \right\rceil, 2n, \left\lfloor \frac{k-2-3n}{2} \right\rfloor, 2+n-k\right)$$

For any such cluster variable, if G is the subgraph of its corresponding contour, then $c(G)$ is the Laurent polynomial of the cluster variable.

Contours for Cluster Variables

To get the desired subgraph, we use 5-sided contours as a tool to cut the brane tiling. Figure 7 shows the fundamental shape of the 5-sided contour and the relation between side lengths.

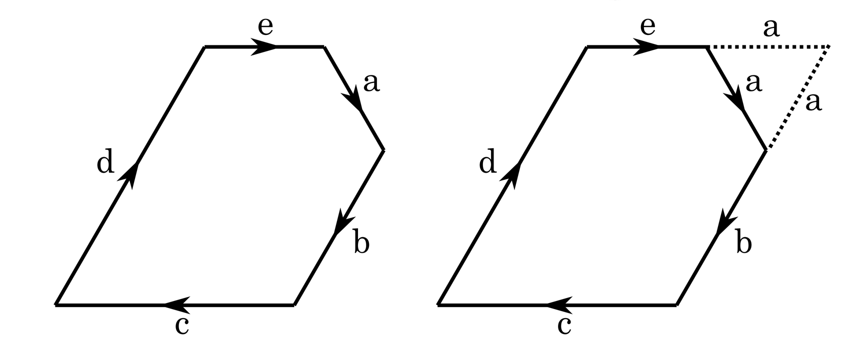

Figure 7: Fundamental Shape of the Contour

Then we define the rule to get a subgraph from a contour. Figure 8 gives an illustration of this rule.

Theorem 5.1. [Rules to Get Subgraph]

- positive length $\to$ keep black points; negative length $\to$ keep white points.
- $b \equiv d \pmod 2$, keep **special** point; $b \not\equiv d \pmod 2$, remove **special** point.

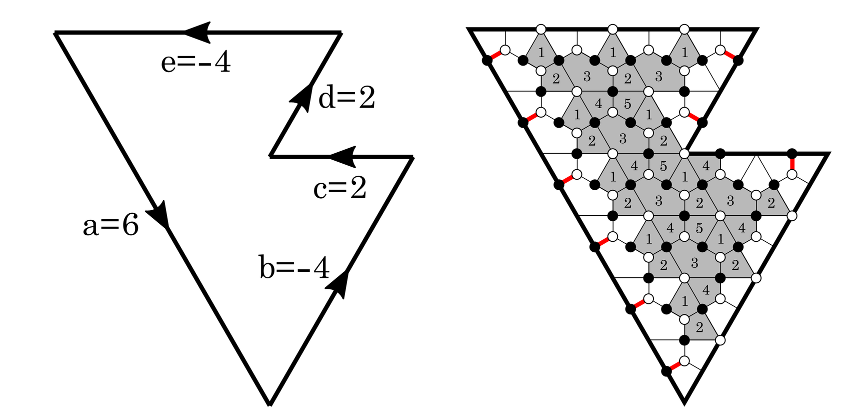

Figure 8: Example of a Subgraph from Contour

Our main theorem gives a formula of the contours. From these contours, we use Theorem 5.1 to get the subgraph, and use Definition 4.1 to recover the cluster variables. The correctness of the main theorem shows that they match the cluster variables stated in Theorem 3.2.

Reference

[1] Tri Lai and Gregg Musiker. Beyond aztec castles: Toric cascades in the dp_3 quiver. *arXiv preprint arXiv:1512.00507*, 2015.

[2] Megan Leoni, Gregg Musiker, Seth Neel, and Paxton Turner. Aztec castles and the dp3 quiver. *Journal of Physics A: Mathematical and Theoretical*, 47(47):474011, 2014.

Acknowledgments

This research was carried out as part of the 2016 REU program at the University of Minnesota, Twin Cities, and was supported by NSF RTG grant DMS-1148634 and by NSF grant DMS-1351590. The authors would like to thank Victor Reiner, Sunita Chepuri and Elise delMas for their advice and comments. The authors are especially grateful to Gregg Musiker for his mentorship, support, and valuable advice.